OPEN ACCESS

University of Dundee

University of Dundee

Methotrexate promotes glucose uptake and lipid oxidation in skeletal muscle via AMPK activation

Pirkmajer, Sergej; Kulkarni, Sameer S.; Tom, Robby Z.; Ross, Fiona A.; Hawley, Simon A.; Hardie, D. Grahame

Published in:
Diabetes

DOI:
10.2337/db14-0508

Publication date:
2015

Document Version
Peer reviewed version

Link to publication in Discovery Research Portal

Citation for published version (APA):
Pirkmajer, S., Kulkarni, S. S., Tom, R. Z., Ross, F. A., Hawley, S. A., Hardie, D. G., Zierath, J. R., & Chibalin, A. V. (2015). Methotrexate promotes glucose uptake and lipid oxidation in skeletal muscle via AMPK activation. *Diabetes*, *64*(2), 360-369. https://doi.org/10.2337/db14-0508

General rights
Copyright and moral rights for the publications made accessible in Discovery Research Portal are retained by the authors and/or other copyright owners and it is a condition of accessing publications that users recognise and abide by the legal requirements associated with these rights.

Take down policy
If you believe that this document breaches copyright please contact us providing details, and we will remove access to the work immediately and investigate your claim.

Download date: 26. Apr. 2025

This is an author-created, uncopyedited electronic version of an article accepted for publication in Diabetes. The American Diabetes Association (ADA), publisher of Diabetes, is not responsible for any errors or omissions in this version of the manuscript or any version derived from it by third parties. The definitive publisher-authenticated version will be available in a future issue of Diabetes in print and online at http://diabetes.diabetesjournals.org.

Methotrexate promotes glucose uptake and lipid oxidation in skeletal muscle via AMPK activation

Sergej Pirkmajer[1*], Sameer S. Kulkarni[1*], Robby Z. Tom[1], Fiona A. Fyffe[2], Simon A. Hawley[2], D. Grahame Hardie[2], Juleen R. Zierath[1,3], and Alexander V. Chibalin[1#]

1) Department of Molecular Medicine and Surgery, Integrative Physiology, Karolinska Institutet, Stockholm, Sweden; 2) Division of Cell Signalling & Immunology, College of Life Sciences, University of Dundee, Scotland, UK; 3) Department of Physiology and Pharmacology, Integrative Physiology, Karolinska Institutet, Stockholm, Sweden.
*These authors have contributed equally to this work

Running title: *Methotrexate enhances AMPK activation*

[#]To whom correspondence should be addressed: Alexander V. Chibalin, Department of Molecular Medicine and Surgery, Integrative Physiology, Karolinska Institutet, SE-171 77 Stockholm, Sweden; Tel +46 8 524 87510; Fax: +46 8 33 54 36; Email: Alexander. Chibalin@ki.se

Abstract: 180 words

Manuscript: 4000 words

References: 49

7 Figures and 1 Table

ABSTRACT

Methotrexate (MTX) is a widely used anti-cancer and anti-rheumatic drug that has been postulated to protect against metabolic risk factors associated with type 2 diabetes mellitus, although the mechanism remains unknown. MTX inhibits 5-aminoimidazole-4-carboxamide ribonucleotide formyltransferase / inosine monophosphate cyclohydrolase (ATIC) and thereby slows down the metabolism of ZMP and its precursor AICAR, which is a pharmacological AMPK activator. We explored whether MTX promotes AMPK activation in cultured myotubes and isolated skeletal muscle. We found MTX markedly reduced the threshold for AICAR-induced AMPK activation, and potentiated glucose uptake and lipid oxidation. Gene silencing of the MTX target ATIC activated AMPK and stimulated lipid oxidation in cultured myotubes. Furthermore, MTX activated AMPK in wild-type HEK-293 cells. These effects were abolished in skeletal muscle lacking the muscle-specific, ZMP-sensitive AMPK-γ3 subunit and in HEK-293 cells expressing a ZMP-insensitive mutant AMPK-γ2 subunit. Collectively, our findings underscore a role for AMPK as a direct molecular link between MTX and energy metabolism in skeletal muscle. Co-therapy with AICAR and MTX could represent a novel strategy to treat metabolic disorders and overcome current limitations of AICAR mono-therapy.

INTRODUCTION

Chronic therapy with methotrexate (MTX), a broadly used anti-cancer and anti-rheumatic drug, may protect rheumatic patients against metabolic risk factors associated with cardiovascular disease, obesity (1) and type 2 diabetes (2). This notion is supported by recent observations that MTX alleviates hyperglycemia and insulin resistance in diabetic (*db/db*) mice (3) and obese mice fed a high-fat diet (4). MTX is a folate antagonist and inhibits DNA replication (5), which explains its anti-cancer action, but the not improvements in glucose homeostasis in type 2 diabetes or obesity. Suppression of chronic inflammation, thought to arise from MTX-stimulated adenosine release (6), may improve glucose homeostasis indirectly (7). Since anti-rheumatic drugs are not invariably associated with metabolic protection (1, 8), other mechanisms are likely. While MTX-induced adenosine release may have direct metabolic effects (4), its exact role is ambiguous, since both adenosine receptor activation (9) and blockage (10) improves insulin sensitivity. Clearly the molecular underpinnings of MTX action in relation to metabolic disease remain undefined.

MTX has several pharmacological targets, including 5-aminoimidazole-4-carboxamide ribonucleotide formyltransferase / inosine monophosphate cyclohydrolase (ATIC) (11). ATIC is essential for the conversion of 5-aminoimidazole-4-carboxamide-1-β-D-ribofuranosyl-5'-monophosphate (ZMP) to inosine monophosphate in the final two steps of the *de novo* purine synthesis pathway. Thus, congenital ATIC deficiency or MTX therapy elevates intracellular ZMP content and excretion of its metabolites (6, 12, 13). The purine precursor ZMP is also an AMP-mimetic and activates the AMP-activated protein kinase (AMPK) (14). AMPK is a heterotrimeric serine-threonine kinase, composed of the catalytic α and non-catalytic β and γ subunits (15). ZMP binds to the AMP-binding sites on the γ subunits (16), and this is required for its ability to activate AMPK (17). AMPK plays a role in maintaining energy homeostasis and is currently a target for the treatment of type 2 diabetes

(18-20). Thus, MTX might mitigate metabolic impairments by promoting ZMP-stimulated AMPK activation in key organs controlling glucose homeostasis.

AMPK activation increases glucose uptake, fatty acid oxidation and mitochondrial biogenesis, which helps to ameliorate different aspects of metabolic dysregulation, including hyperglycemia and insulin resistance (19). MTX could promote ZMP accumulation and AMPK activation by suppressing ATIC, which is expressed and active in skeletal muscle (21, 22). ZMP is also the active metabolite of the pharmacological AMPK activator 5-aminoimidazole-4-carboxamide-1-β-D-ribofuranoside (AICAR) (14). AICAR therapy promotes favorable metabolic reprogramming in skeletal muscle of sedentary (23) and diabetic (*ob/ob*) mice (24). However, a relatively high threshold for AMPK activation (25), in conjunction with poor bioavailability (26), limits the usefulness of AICAR in the treatment of type 2 diabetes (27). MTX may enhance AICAR-stimulated AMPK activation in skeletal muscle by suppressing ATIC-mediated ZMP clearance and overcome this problem.

Here, we show that MTX markedly reduces the threshold for AICAR-stimulated AMPK activation and potentiates glucose uptake and lipid oxidation in skeletal muscle. Thus, co-therapy with AICAR and MTX could represent a novel strategy to treat metabolic disorders and overcome current limitations of AICAR mono-therapy.

METHODS

Antibodies and reagents

Antibodies against phospho-AMPKα (Thr^{172}) and phospho-ACC (Ser^{79}) were from Cell Signaling Technology (Beverly, MA), the antibody against ATIC was from Sigma-Aldrich (Stockholm, Sweden), the GLUT4 antibody was from Millipore (Temecula, CA), and the antibody against GAPDH was from Santa Cruz Biotechnology (Santa Cruz, CA). ECL reagent and the protein molecular weight marker were from GE Healthcare (Uppsala,

Sweden). BCA Protein Assay kit was from Pierce (Rockford, IL), and PVDF Immobilon-P membrane from Millipore (Bedford, MA). Cell culture materials were from Costar (Täby, Sweden). [9-10(n)-^{3}H]-palmitic acid and [1,2-^{3}H]-2-deoxy-D-glucose were from Perkin-Elmer. All other reagents, unless otherwise specified, were of analytical grade and obtained from Sigma-Aldrich (Stockholm, Sweden).

L6 cells and siRNA transfection

L6 muscle cells were grown in αMEM supplemented with 10% fetal bovine serum (FBS), 1% PeSt (100 U/ml penicillin and 100 µg/ml streptomycin), and 1% Fungizone at 37°C in humidified air/5% CO_2. They were differentiated into myotubes in αMEM (2% FBS, 1% PeSt and 1% Fungizone). L6 cells were transfected with a pool of siRNAs (100 nM) against ATIC mRNA or scrambled siRNA (Dharmacon; Chicago, IL) using CellPhect Transfection Kit on days 2 and 4 of differentiation. Experiments were performed 48–72 hours after the last transfection.

Primary human skeletal muscle cells

Primary human skeletal muscle myoblasts were from Lonza Group Ltd (Basel, Switzerland) and maintained in DMEM/F12 supplemented with 20% FBS, 1% PeSt and 1% Fungizone at 37°C in humidified air/7% CO_2. Myoblasts were differentiated into myotubes for 5 days in DMEM (2% FBS, 1% PeSt and 1% Fungizone). Serum-starved myotubes were incubated for 4 hours and subsequently with or without 5 µM MTX and/or 0.2 mM AICAR for 5 hours.

Metabolic assays in L6 myotubes

L6 myotubes were incubated in αMEM (w/o nucleosides) with or without 5 µM MTX for 16 hours prior to the experiment. For fatty acid oxidation, myotubes were serum-starved for 4 hours and then incubated with or without MTX (5 µM) and/or AICAR (0.2 or 2 mM) for 5 hours in αMEM, supplemented with 0.2% BSA, 20 µM cold palmitate and 0.5 µCi/ml [^{3}H]-palmitic acid. Palmitate oxidation was determined by measuring the amount of $^{3}H_2O$ in cell

culture media. Non-metabolized palmitate was adsorbed to charcoal and removed by centrifugation (16,000 rpm, 15 minutes). For glucose uptake, L6 myotubes were incubated with or without MTX (5 μM) and/or AICAR (0.2 mM or 2 mM) in serum-free αMEM (w/o nucleosides) for 5 hours. Myotubes were then washed with HBS (140 mM NaCl, 20 mM Hepes, 5 mM KCl, 2.5 mM $MgSO_4$, 1 mM $CaCl_2$, pH 7.4) and subsequently incubated in HBS supplemented with 10 μM 2-deoxy-D-glucose and 0.75-1 μCi/ml [1,2-^{3}H]-2-deoxy-D-glucose for 10 minutes. Nonspecific glucose transport was assessed in the presence of 10 μM cytochalasin B. Myotubes were then washed with ice-cold stop solution (25 mM glucose, 0.9% (w/v) NaCl) and lysed in 0.03% (w/v) SDS. Radioactivity was measured in cell lysates by liquid scintillation counting.

Experimental animals

This study was approved by the Regional Animal Ethical Committee (Stockholm, Sweden). AMPK-γ3 knock-out (AMPK-γ3$^{-/-}$) mice were bred onto a C57BL/6 genetic background and have been thoroughly characterized (28). Prior to all experiments, AMPK-γ3$^{-/-}$ and wild-type mice were fasted for 4 hours before being anesthetized with Avertin (0.02 ml/g i.p.).

Metabolic assays in isolated skeletal muscle

Extensor digitorum longus (EDL) and soleus muscle from wild-type or AMPK-γ3$^{-/-}$ mice were preincubated at 30°C in oxygenated (95% O_2/5% CO_2) Krebs-Henseleit bicarbonate buffer (KHB) supplemented with 5 mM glucose, 15 mM mannitol, 5 mM HEPES and 0.1% (w/v) BSA with or without 10 μM MTX for 2 hours. Thereafter, muscles were incubated for 2-hour with or without 10 μM MTX and/or AICAR (0.2 mM or 2 mM). Glucose transport was assessed by measuring the uptake of [1,2-^{3}H]-2-deoxy-D-glucose as described (28). Muscles were incubated in KHB supplemented with 1 mM 2-deoxy-D-glucose, 19 mM of mannitol, 2.5 μCi/ml of [1,2-^{3}H]-2-deoxy-D-glucose and 0.7 μCi/ml of [^{14}C] mannitol for 20 minutes. For fatty acid oxidation, KHB was supplemented with [H^3]-palmitic acid (0.4 μCi/ml) and 0.3

mM cold palmitate and oxidation was determined by analyzing the [^{3}H]-labeled water content using liquid scintillation counting as described above.

Lysate preparation and immunoblot analysis

Myotubes were washed with ice-cold PBS and lysed in homogenization buffer (1% Protease Inhibitor Cocktail, 137 mM NaCl, 2.7 mM KCl, 1 mM $MgCl_2$, 5 mM $Na_4P_2O_7$, 0.5 mM Na_3VO_4, 1% Triton X-100, 10% glycerol, 20 mM Tris, 10 mM NaF, 1 mM EDTA and 0.2 mM phenylmethylsulfonyl fluoride, pH 7.8). Lysates were subjected to centrifugation for 15 minutes at 12,000 x g (4°C). Muscle was homogenized in ice-cold buffer, followed by end-over-end rotation for 60 minutes (4°C) and centrifugation at 12,000 x g for 10 minutes (4°C). Supernatants of cell or muscle lysates were collected and protein content was measured (BCA Protein Assay). Proteins dissolved in Laemmli buffer (25µg per well) were resolved on 4-12% Bis-Tris gel (Bio-Rad, Richmond, CA), transferred to PVDF membrane and blocked with 7.5% non-fat milk and probed overnight (4^{o}C) with primary antibodies. All primary antibodies were diluted 1:1,000 in primary antibody buffer (Tris-buffered saline (TBS), 0.5% BSA, 0.5% NaN_3, pH 7.6). Following the overnight incubation, membranes were washed with washing buffer (TBS, 0.02% Tween-20) and incubated with appropriate horseradish peroxidase-conjugated secondary antibodies (Bio-Rad) for 1 hour at room temperature. The secondary antibodies were diluted 1:25,000 in TBS supplemented with 5% non-fat milk. Immunoreactive proteins were visualized by enhanced chemiluminiscence and quantified by the Quantity One 1-D Analysis Software (Bio-Rad). Data were normalized to GAPDH.

Plasmids and generation of stable wild-type and R531G AMPK-γ2 HEK-293 cell lines

Full-length human γ2 was amplified with primers designed to encode a 5'-BamHI site and a C-terminal FLAG tag followed by an XhoI site. The resulting PCR product was cloned into the pcDNA5/FRT/TO plasmid (Invitrogen) to create pcDNA5/FRT/TO/g2. Mutagenesis of the construct was performed using the QuikChange Site-Directed Mutagenesis system

(Stratagene). The plasmid (POG44) expressing Flp recombinase was from Invitrogen. T-Rex HEK-293 cells containing a single FRT site (Invitrogen) were transfected with Fugene6 (Promega) using the plasmids POG44 and pcDNA5/FRT/TO/g2 at a ratio of 9:1. Fresh medium was added to the cells 24 hours after transfection, and media containing 200 μg/ml hygromycin B and 15 μg/ml blasticidin was added 48 hours after transfection. The medium was replaced every 3 days until foci could be identified, and individual foci were then selected and expanded. The expression of FLAG-tagged g2 was induced by adding 1 μg/ml tetracycline for 40 hours, and expression detected using immunofluorescence microscopy and Western blot using anti-FLAG antibodies.

Culture of wild-type and R531G AMPK-γ2 HEK-293 cells and cell treatments

HEK-293 cells expressing wild-type or R531G AMPK-γ2 were generated as described (17). T-Rex-Flp-In HEK-293 cells (Invitrogen) containing a single FRT site were cultured in Dulbecco's modified Eagle's medium (DMEM) containing 4.5 g/L glucose, 10% (v/v) FBS, 100 IU/ml penicillin, 100 μg/ml streptomycin, 15 μg/ml blasticidin and 100 μg/ml zeocin. After transfection, T-Rex-Flp-In HEK-293 cells stably expressing either WT or R531G AMPK-γ2 were cultured as above except that zeocin was replaced by 200 μg/ml hygromycin B. Forty hours after the induction of protein, 3 μM MTX/DMSO was added to cells for 16 hours, followed by 1 hour of AICAR in different concentrations.

AMPK activity assays

Wild-type HEK-293 cells or RG cells were assayed for AMPK activity as described (17). Activity of the purified rat liver AMPK, which is approximately an equal mixture of the α1β1γ1 and α2β1γ1 heterotrimer (29), was measured in the presence or absence of AMP or PP2C as described (30).

Statistics

Results are presented as means±SEM or means±SD. Comparisons between multiple groups were performed using ANOVA, followed by Bonferroni's or Dunnett's *post hoc* test. Student's t-test was used when two groups were compared. Statistical significance was established at $P<0.05$.

RESULTS

MTX promotes AMPK activation in cultured myotubes

To determine whether MTX modulates AMPK activation, L6 myotubes and primary human myotubes were exposed to 5 μM MTX and sub-threshold (0.2 mM) and/or maximally effective (2 mM) concentrations of AICAR (14, 25). AMPK activation was determined by measuring AMPK Thr^{172} and acetyl-CoA carboxylase Ser^{79} (ACC) phosphorylation. Exposure of cultured myotubes to 0.2 mM AICAR alone did not elevate AMPK or ACC phosphorylation (Fig. 1A-D), demonstrating that 0.2 mM AICAR is below the threshold for AMPK activation. Conversely, co-incubation with MTX and 0.2 mM AICAR robustly increased phosphorylation of AMPK (Fig. 1A, B) and ACC (Fig. 1C, D), demonstrating MTX markedly reduces the threshold for AMPK activation.

MTX promotes metabolic effects in skeletal muscle via AMPK activation

To investigate whether the augmented AICAR-stimulated ACC phosphorylation in MTX-treated myotubes translates into increased lipid utilization, palmitate oxidation was measured in L6 myotubes incubated with 5 μM MTX and/or AICAR (0.2 or 2 mM). While 0.2 mM AICAR alone failed to increase palmitate oxidation, treatment with 0.2 mM AICAR and MTX together stimulated palmitate oxidation in L6 myotubes (Fig. 2A).

We next examined whether AICAR-stimulated glucose uptake is augmented in L6 myotubes after exposure to 5 μM MTX (Fig. 2B). Although exposure of L6 myotubes to 0.2 mM AICAR alone failed to stimulate glucose uptake, a combined treatment with 0.2 mM AICAR and MTX markedly elevated glucose uptake. MTX enhanced glucose uptake in myotubes treated with saturating concentration of AICAR (2 mM), indicating AICAR responsiveness was improved. Glucose transport was also determined in EDL and soleus muscle treated with 2 mM AICAR and/or 10 μM MTX (Fig. 2C). MTX robustly augmented AICAR-stimulated glucose uptake in EDL muscle, underscoring the effect of MTX to

potentiate AICAR responsiveness. Although soleus muscle was less responsive to AICAR, glucose uptake was elevated upon MTX and AICAR exposure. MTX treatment did not affect GLUT4 protein abundance or GLUT4 mRNA expression (data not shown).

MTX promotes AMPK activation through indirect mechanisms

To confirm that MTX treatment inhibited ATIC, ZMP content was measured in L6 cells exposed to 0.2 mM AICAR and/or 5 μM MTX. AICAR alone did not elevate ZMP content, indicative of the high ZMP turnover (Fig.3A). However, a combined treatment with MTX and 0.2 mM AICAR robustly increased the ZMP:ATP ratio. MTX exposure suppresses *de novo* purine synthesis (31) and may provoke ATP depletion in some situations (32, 33). ATP depletion decreases adenylate energy charge (Table 1), which stimulates AMPK activation directly (34). Given that the AMP concentration in cultured myotubes was too low for reliable quantitative estimation of energy charge, we determined the ADP:ATP ratio as a marker of cellular energy status (17). MTX exposure, in the absence or presence of AICAR, increased the ADP:ATP ratio 24-28% (Fig. 3B), indicating a modest degree of energy stress. The observed increases in the ZMP content and the ADP:ATP ratio provide evidence that MTX promotes AMPK activation in cultured myotubes primarily by decreasing ZMP clearance, although ATP depletion may play a secondary role.

To establish a causal link between MTX-induced alterations in cellular nucleotide content and AMPK activation, wild-type HEK-293 and mutant HEK-293 (RG) cell lines were exposed to MTX (3 μM) and different concentrations of AICAR (Fig. 3C-F). RG cells harbor a single substitution (R531G) within the AMPK-γ2 subunit, which renders AMPK insensitive to stimulation by AMP and ZMP (17). Both ZMP content and the ADP:ATP ratio were increased in wild-type cells treated with MTX and AICAR (Fig. 3C, D). The elevated ZMP content during MTX and AICAR treatment was paralleled by an increase in AMPK activity (Fig. 3E). Notably, MTX alone was sufficient to activate AMPK in wild-type cells.

However, the increase in AMPK activity was almost entirely abrogated in RG cells during co-incubation with MTX and AICAR (Fig. 3F), and MTX alone did not stimulate AMPK activation in RG cells. Since AMPK complexes in RG cells remain responsive to direct AMPK activators other than AMP and ZMP such as A-769662 (17), this suggests that MTX is not a direct AMPK activator.

MTX is not a direct AMPK activator

To evaluate whether MTX activates AMPK allosterically, the activity of AMPK, purified from rat liver, was measured during incubation with AMP and/or increasing concentrations of MTX (Fig. 4A). AMPK activity was increased in the presence of 200 μM AMP, but MTX alone or in combination with AMP did not alter AMPK activity. We also determined whether MTX protects AMPK from dephosphorylation by protein phosphatase 2C (PP2C), which dephosphorylates and thereby inactivates AMPK (35). Purified AMPK was incubated with PP2C and either 200 μM AMP or different concentrations of MTX (Fig. 4B). AMP almost completely prevented the inactivation of AMPK by PP2C, but MTX did not, showing that MTX does not inhibit PP2C-mediated dephosphorylation of AMPK.

MTX is dependent on AMPK to promote lipid oxidation

Our results have established that MTX enhances AICAR action in skeletal muscle. To determine whether MTX depends on AMPK to promote metabolic alterations in skeletal muscle, we studied EDL and soleus muscles from wild-type and AMPK-$\gamma3^{-/-}$ knock-out mice. Isolated EDL and soleus muscles were incubated in the absence or presence of 10 μM MTX and/or a sub-threshold concentration of AICAR (0.2 mM). Treatment with 0.2 mM AICAR and MTX was sufficient to markedly stimulate AMPK activation and palmitate oxidation in wild-type EDL and soleus muscles (Fig. 5). However, co-incubation with MTX and 0.2 mM AICAR did not stimulate phosphorylation of AMPK (Fig. 5A) and ACC (Fig. 5C) in AMPK-$\gamma3^{-/-}$ EDL muscle. MTX also failed to enhance AICAR-stimulated palmitate oxidation in

AMPK-γ3$^{-/-}$ EDL muscle (Fig. 5E), supporting the notion that MTX promotes these metabolic alterations through AMPK. Due to low expression of AMPK-γ3 in wild-type soleus muscle (36), the response to a combined treatment with MTX and 0.2 mM AICAR was similar between soleus muscles from wild-type and AMPK-γ3$^{-/-}$ mice (Fig. 5B, D, F).

To establish whether MTX promotes AMPK activation by decreasing ZMP clearance, nucleotide content was measured. ZMP content was markedly elevated upon addition of AICAR in wild-type EDL and soleus muscle (Table 1). Although MTX markedly augmented AICAR-stimulated AMPK activation and palmitate utilization, it did not enhance ZMP accumulation in EDL and soleus muscle. Adenylate energy charge also remained unaltered upon MTX treatment (Table 1). These results suggest that diminished ZMP clearance and/or energy depletion are not the exclusive mechanisms underlying an MTX-induced reduction in the threshold for AICAR-stimulated AMPK activation in skeletal muscle.

Suppression of ATIC directly promotes AMPK activation and increases lipid oxidation

L6 myotubes were utilized to validate ATIC as an MTX target (Fig. 6A). Expression of ATIC was suppressed in L6 myotubes using siRNA (Fig. 6B). Exposure of myotubes transfected with scrambled siRNA to 0.2 mM AICAR did not increase ZMP content (Fig. 6C). Conversely, stimulation with 0.2 mM AICAR robustly elevated ZMP content in ATIC-depleted myotubes (Fig. 6C), indicating diminished ZMP clearance. The ADP:ATP ratio was also elevated 12-15% in ATIC-depleted cells (Fig. 6D), possibly reflecting purine depletion due to decreased *de novo* synthesis. The increased ZMP content in ATIC-depleted myotubes treated with AICAR increased AMPK and ACC phosphorylation and palmitate oxidation (Fig. 6E-G), consistent with the hypothesis that decreased ZMP clearance promotes AMPK activation. Notably, ATIC depletion alone increased AMPK phosphorylation and palmitate oxidation (Fig. 6E, G), underscoring the link between ATIC suppression and AMPK activation in skeletal muscle.

Gene silencing suppressed ATIC expression 70% (Fig. 6B). To test whether inhibition of residual ATIC activity provides an additional stimulus for AMPK activation, L6 myotubes were transfected with siRNA and subsequently exposed to MTX and incubated in the presence of 0.2 mM AICAR. In ATIC-depleted myotubes, MTX robustly stimulated AMPK and ACC phosphorylation, as well as palmitate oxidation (Fig. 6H-J). ATIC depletion in conjunction with MTX exposure achieved maximal AMPK activation, since incubation with 0.2 mM AICAR failed to exert an additional effect. However, a combined treatment with 0.2 mM AICAR and MTX triggered a similar response in control myotubes transfected with scrambled siRNA.

DISCUSSION

Epidemiological (1, 2) and experimental (3, 4) evidence suggest that MTX may protect against type 2 diabetes, but the underlying mechanisms have been unclear. We provide evidence that MTX potentiates AICAR-stimulated AMPK activation and glucose uptake and lipid oxidation in skeletal muscle. We also demonstrate that suppression of ATIC, a well-characterized MTX target (11), directly promotes AMPK activation in cultured myotubes. Finally, MTX alone is sufficient to stimulate AMPK activation in HEK-293 cells. These results highlight a role for AMPK as link between MTX and skeletal muscle energy metabolism.

Pharmacological activation of AMPK in skeletal muscle represents a promising strategy to bypass insulin-resistant pathways, in order to stimulate glucose uptake and improve insulin sensitivity in type 2 diabetes (19). However, the search for peripheral AMPK activators has been challenging. AMPK activators, such as A-769662, target AMPK-β1 complexes that are poorly expressed in skeletal muscle (37, 38), whereas AICAR has clinical limitations due to its poor bioavailability (18, 26). Even with intravenous infusion, the plasma

concentration of AICAR (0.16-0.18 mM) remains below the threshold for AMPK activation in skeletal muscle (27, 39). Here we report co-incubation with 0.2 mM AICAR and MTX activates AMPK and stimulates glucose uptake and lipid oxidation in skeletal muscle. These results are consistent with effects of MTX on AICAR in cancer cells (32). Thus, combined therapy with MTX and AICAR might provide a novel pharmacological strategy to overcome current limitations of AICAR mono-therapy.

AMPK-γ3 is the muscle-specific isoform of the AMP- and ZMP-sensitive AMPK-γ subunit, which exists in three isoforms (γ1-γ3) (40), and a major isoform involved in exercise-induced AMPK activation (41). Although AMPK-γ3 is expressed primarily in glycolytic muscles (28, 36), a complete failure of MTX to enhance AICAR action in AMPK-$\gamma3^{-/-}$ EDL muscle was unexpected since AMPK-γ1 and -γ2 isoforms are also expressed (36). Furthermore, MTX enhanced AICAR-stimulated AMPK phosphorylation in wild-type and AMPK-$\gamma3^{-/-}$ soleus muscle, despite low endogenous expression in wild-type soleus muscle (28, 36). Thus, in glycolytic skeletal muscle, MTX preferentially promotes activation of AMPK-γ3-containing complexes. The γ3 subunit offers an entry point to tissue-specific regulation of AMPK function, and a possible therapeutic target for treatment of insulin resistance in type 2 diabetes (28). Activating mutations in the γ3 isoform are associated with skeletal muscle remodeling analogous to exercise training, including augmented mitochondrial biogenesis, and fat oxidation, as well as protection against insulin resistance (28, 42). Co-therapy with MTX and AICAR may therefore promote a plethora of beneficial metabolic alterations, including mimicking the effects of exercise training (23).

MTX promotes AMPK activation in cultured myotubes and WT cells primarily via inhibition of ATIC, while ATP depletion may also have a secondary role. However, MTX did not inhibit ATIC or evoke energy depletion in murine EDL and soleus muscles, although AICAR action was markedly enhanced. This failure to suppress ATIC activity may be

explained by the fact that MTX is an efficient ATIC inhibitor only after MTX polyglutamates are formed by the action of folylpolyglutamate synthetase, which is a slow process (11). Thus, the exposure time during the isolated skeletal muscle incubation may have been insufficient for MTX to depress ATIC activity. While our data do not exclude a role for ATIC inhibition during chronic MTX therapy, they nevertheless suggest that MTX promotes AMPK activation through additional, ATIC-independent mechanisms. This ATIC-independent pathway appears to be operate independent of any activation of up-stream kinases like LKB1, which phosphorylate AMPK at Thr^{172} (15). Indeed, MTX alone failed to activate AMPK in RG cells, although they are normally responsive to AMPK activators other than ZMP and AMP (17). However, MTX decreases the concentration of S-adenosylmethionine (43), a biological methyl group donor that promotes AMPK inactivation (44), which may provide one possible ATIC-independent pathway.

MTX has several targets aside from ATIC (11), which may also modulate AMPK activation. In particular, the activity of glycinamide ribonucleotide transformylase (GART), an enzyme upstream of ATIC in the *de novo* pathway of purine synthesis (Fig. 7), may critically determine the level of endogenous ZMP. Concurrent inhibition of ATIC and GART by MTX suppresses the entire *de novo* synthesis pathway and decreases endogenous ZMP formation (31). This provides a possible explanation why MTX alone did not increase the content of endogenous ZMP in cultured myotubes, although the clearance of ZMP derived from AICAR was decreased. Similarly, MTX increases ZMP content and enhances AMPK activation in AICAR-treated cancer cells, but not when used alone (32). Conversely, ATIC depletion elevated basal AMPK phosphorylation and palmitate oxidation in cultured myotubes, suggesting selective inhibition of ATIC in skeletal muscle may introduce a metabolic block leading to ZMP accumulation and AMPK activation.

MTX has a greater propensity to inhibit ATIC than GART (11, 31). Patients receiving low-dose MTX exhibit increased urinary excretion of 5-aminoimidazole-4-carboxamide (13), a ZMP degradation product, which is indicative of ZMP accumulation due to ATIC inhibition. Conversely, high-dose MTX fails to increase urinary excretion of endogenous AICAR (45). Scaling down MTX dosage may create a therapeutic window for more selective ATIC inhibition with subsequent ZMP accumulation and AMPK activation in skeletal muscle and other metabolic tissues. Consistent with this hypothesis, low-dose MTX therapy increased intracellular ZMP content in mice (6). Furthermore, low-dose MTX mono-therapy increases skeletal muscle GLUT4 abundance in diabetic (*db/db*) mice (3) and suppresses adipose tissue lipolysis in obese mice (4), consistent with AMPK activation in skeletal muscle (24, 46) and adipose tissue (14), respectively. Finally, we report MTX alone is sufficient to induce AMPK activation in HEK-293 cells, thus providing proof of concept that MTX acts as AMPK activator, rather than just as an enhancer of effects of AICAR.

We show that MTX enhances AICAR-stimulated AMPK activation in skeletal muscle as well as in cells of kidney origin (HEK-293 cells). Taken together with studies in different types of cancer cells (31, 32), these data suggest that MTX potentiates effects of AICAR not only in skeletal muscle, but also in other organs. For instance, ATIC is expressed and active in heart (21, 47), indicating MTX could enhance AICAR action in cardiomyocytes. Also, liver expresses ATIC (47) and MTX-treated hepatic carcinoma cells release adenosine (48), which results from MTX-induced ATIC inhibition (6). Consistent with the involvement of ATIC, we determined that MTX enhances ZMP accumulation and AMPK activation in AICAR-treated H4IIE cells of liver origin (data not shown). Aside from ATIC expression, differences in MTX uptake might also determine tissue responsiveness to co-therapy with AICAR and MTX. Indeed, cells lacking MTX transporters are resistant to MTX despite ATIC

expression (32, 49). Collectively, these studies indicate that MTX is likely to enhance AICAR action in all tissues that express ATIC and MTX uptake transporters.

In conclusion, MTX markedly reduces the threshold for AICAR-induced AMPK activation and increases glucose uptake and lipid oxidation in skeletal muscle. The underlying mechanisms include reduced ZMP clearance due to ATIC inhibition and ATP depletion, as well as ATIC-independent effects. Collectively, our results highlight a role for AMPK as a direct link between MTX and energy metabolism. Co-therapy with AICAR and MTX or another MTX-based agent represents a novel strategy to treat metabolic disorders and overcome current limitations of AICAR mono-therapy.

ACKNOWLEDGMENTS

S.P, D.G.H, J.R.Z and A.V.C. designed the study; S.P, S.S.K, R.Z.T., F.A.F. and S.A.H. performed experiments; S.P., J.R.Z. and A.V.C. wrote the manuscript; D.G.H., J.R.Z. and A.V.C. revised the final manuscript, S.P, S.S.K, R.Z.T., F.A.F., D.G.H., J.R.Z. and A.V.C approved the final manuscript. A.V.C. is the guarantor of this work and, as such, had full access to all the data in the study and takes responsibility for the integrity of the data and the accuracy of the data analysis.

We would like to thank Dr. Megan E. Osler (Karolinska Institutet) for critical reading of the manuscript and Dr. Amira Klip (The Hospital for Sick Children, Toronto, Canada) for generously providing the L6 muscle cells. This study was supported with funding from the European Research Council Ideas Program (ICEBERG, ERC-2008-AdG23285), Swedish Research Council, Swedish Diabetes Association, Strategic Research Foundation, Novo Nordisk Research Foundation, the Commission of the European Communities (Contract No LSHM-CT-2004-005272 EXGENESIS) and the Strategic Research Programme in Diabetes at Karolinska Institutet. Studies in the Hardie laboratory are supported by a Senior Investigator Award (097726) from the Wellcome Trust and by a Programme Grant (C37030/A15101) from Cancer Research UK. S. P. was supported by the Slovenian Research Agency (Grant P3-0043) and the LPP/Erasmus program.

The authors report no potential conflicts of interest relevant to this article.

REFERENCES

1. Toms, T.E., Panoulas, V.F., John, H., Douglas, K.M., and Kitas, G.D. 2009. Methotrexate therapy associates with reduced prevalence of the metabolic syndrome in rheumatoid arthritis patients over the age of 60- more than just an anti-inflammatory effect? A cross sectional study. *Arthritis Res Ther* 11:R110.

2. Solomon, D.H., Massarotti, E., Garg, R., Liu, J., Canning, C., and Schneeweiss, S. 2011. Association between disease-modifying antirheumatic drugs and diabetes risk in patients with rheumatoid arthritis and psoriasis. *JAMA* 305:2525-2531.

3. Russo, G.T., Minutoli, L., Bitto, A., Altavilla, D., Alessi, E., Giandalia, A., Romeo, E.L., Stagno, M.F., Squadrito, F., Cucinotta, D., et al. 2012. Methotrexate Increases Skeletal Muscle GLUT4 Expression and Improves Metabolic Control in Experimental Diabetes. *J Nutr Metab* 2012:132056.

4. DeOliveira, C.C., Acedo, S.C., Gotardo, E.M., Carvalho Pde, O., Rocha, T., Pedrazzoli, J., Jr., and Gambero, A. 2012. Effects of methotrexate on inflammatory alterations induced by obesity: an in vivo and in vitro study. *Mol Cell Endocrinol* 361:92-98.

5. Mathews, C.K. 2012. DNA synthesis as a therapeutic target: the first 65 years. *FASEB J* 26:2231-2237.

6. Cronstein, B.N., Naime, D., and Ostad, E. 1993. The antiinflammatory mechanism of methotrexate. Increased adenosine release at inflamed sites diminishes leukocyte accumulation in an in vivo model of inflammation. *J Clin Invest* 92:2675-2682.

7. Svenson, K.L., Pollare, T., Lithell, H., and Hallgren, R. 1988. Impaired glucose handling in active rheumatoid arthritis: relationship to peripheral insulin resistance. *Metabolism* 37:125-130.

8. Hoes, J.N., van der Goes, M.C., van Raalte, D.H., van der Zijl, N.J., den Uyl, D., Lems, W.F., Lafeber, F.P., Jacobs, J.W., Welsing, P.M., Diamant, M., et al. 2011. Glucose tolerance, insulin sensitivity and beta-cell function in patients with rheumatoid arthritis treated with or without low-to-medium dose glucocorticoids. *Ann Rheum Dis* 70:1887-1894.

9. Dhalla, A.K., Wong, M.Y., Voshol, P.J., Belardinelli, L., and Reaven, G.M. 2007. A1 adenosine receptor partial agonist lowers plasma FFA and improves insulin resistance induced by high-fat diet in rodents. *Am J Physiol Endocrinol Metab* 292:E1358-1363.

10. Xu, B., Berkich, D.A., Crist, G.H., and LaNoue, K.F. 1998. A1 adenosine receptor antagonism improves glucose tolerance in Zucker rats. *Am J Physiol* 274:E271-279.

11. Chabner, B.A., Allegra, C.J., Curt, G.A., Clendeninn, N.J., Baram, J., Koizumi, S., Drake, J.C., and Jolivet, J. 1985. Polyglutamation of methotrexate. Is methotrexate a prodrug? *J Clin Invest* 76:907-912.

12. Marie, S., Heron, B., Bitoun, P., Timmerman, T., Van Den Berghe, G., and Vincent, M.F. 2004. AICA-ribosiduria: a novel, neurologically devastating inborn error of purine biosynthesis caused by mutation of ATIC. *Am J Hum Genet* 74:1276-1281.

13. Luhby, A.L., and Cooperman, J.M. 1962. Aminoimidazolecarboxamide excretion in vitamin-B12 and folic-acid deficiencies. *Lancet* 2:1381-1382.

14. Corton, J.M., Gillespie, J.G., Hawley, S.A., and Hardie, D.G. 1995. 5-aminoimidazole-4-carboxamide ribonucleoside. A specific method for activating AMP-activated protein kinase in intact cells? *Eur J Biochem* 229:558-565.

15. Hardie, D.G., Ross, F.A., and Hawley, S.A. 2012. AMPK: a nutrient and energy sensor that maintains energy homeostasis. *Nat Rev Mol Cell Biol* 13:251-262.

16. Day, P., Sharff, A., Parra, L., Cleasby, A., Williams, M., Horer, S., Nar, H., Redemann, N., Tickle, I., and Yon, J. 2007. Structure of a CBS-domain pair from the regulatory gamma1 subunit of human AMPK in complex with AMP and ZMP. *Acta Crystallogr D Biol Crystallogr* 63:587-596.

17. Hawley, S.A., Ross, F.A., Chevtzoff, C., Green, K.A., Evans, A., Fogarty, S., Towler, M.C., Brown, L.J., Ogunbayo, O.A., Evans, A.M., et al. 2010. Use of cells expressing gamma subunit variants to identify diverse mechanisms of AMPK activation. *Cell Metab* 11:554-565.

18. Fogarty, S., and Hardie, D.G. 2010. Development of protein kinase activators: AMPK as a target in metabolic disorders and cancer. *Biochim Biophys Acta* 1804:581-591.

19. Long, Y.C., and Zierath, J.R. 2006. AMP-activated protein kinase signaling in metabolic regulation. *J Clin Invest* 116:1776-1783.

20. Hardie, D.G. 2013. AMPK: a target for drugs and natural products with effects on both diabetes and cancer. *Diabetes* 62:2164-2172.

21. Sabina, R.L., Kernstine, K.H., Boyd, R.L., Holmes, E.W., and Swain, J.L. 1982. Metabolism of 5-amino-4-imidazolecarboxamide riboside in cardiac and skeletal muscle. Effects on purine nucleotide synthesis. *J Biol Chem* 257:10178-10183.

22. Bonsdorff, T., Gautier, M., Farstad, W., Ronningen, K., Lingaas, F., and Olsaker, I. 2004. Mapping of the bovine genes of the de novo AMP synthesis pathway. *Anim Genet* 35:438-444.

23. Narkar, V.A., Downes, M., Yu, R.T., Embler, E., Wang, Y.X., Banayo, E., Mihaylova, M.M., Nelson, M.C., Zou, Y., Juguilon, H., et al. 2008. AMPK and PPARdelta agonists are exercise mimetics. *Cell* 134:405-415.

24. Song, X.M., Fiedler, M., Galuska, D., Ryder, J.W., Fernstrom, M., Chibalin, A.V., Wallberg-Henriksson, H., and Zierath, J.R. 2002. 5-Aminoimidazole-4-carboxamide ribonucleoside treatment improves glucose homeostasis in insulin-resistant diabetic (ob/ob) mice. *Diabetologia* 45:56-65.

25. Merrill, G.F., Kurth, E.J., Hardie, D.G., and Winder, W.W. 1997. AICA riboside increases AMP-activated protein kinase, fatty acid oxidation, and glucose uptake in rat muscle. *Am J Physiol* 273:E1107-1112.

26. Dixon, R., Gourzis, J., McDermott, D., Fujitaki, J., Dewland, P., and Gruber, H. 1991. AICA-riboside: safety, tolerance, and pharmacokinetics of a novel adenosine-regulating agent. *J Clin Pharmacol* 31:342-347.

27. Boon, H., Bosselaar, M., Praet, S.F., Blaak, E.E., Saris, W.H., Wagenmakers, A.J., McGee, S.L., Tack, C.J., Smits, P., Hargreaves, M., et al. 2008. Intravenous AICAR administration reduces hepatic glucose output and inhibits whole body lipolysis in type 2 diabetic patients. *Diabetologia* 51:1893-1900.

28. Barnes, B.R., Marklund, S., Steiler, T.L., Walter, M., Hjalm, G., Amarger, V., Mahlapuu, M., Leng, Y., Johansson, C., Galuska, D., et al. 2004. The 5'-AMP-activated protein kinase gamma3 isoform has a key role in carbohydrate and lipid metabolism in glycolytic skeletal muscle. *J Biol Chem* 279:38441-38447.

29. Woods, A., Salt, I., Scott, J., Hardie, D.G., and Carling, D. 1996. The alpha1 and alpha2 isoforms of the AMP-activated protein kinase have similar activities in rat liver but exhibit differences in substrate specificity in vitro. *FEBS Lett* 397:347-351.

30. Hawley, S.A., Fullerton, M.D., Ross, F.A., Schertzer, J.D., Chevtzoff, C., Walker, K.J., Peggie, M.W., Zibrova, D., Green, K.A., Mustard, K.J., et al. 2012. The ancient drug salicylate directly activates AMP-activated protein kinase. *Science* 336:918-922.

31. Bokkerink, J.P., Bakker, M.A., Hulscher, T.W., De Abreu, R.A., and Schretlen, E.D. 1988. Purine de novo synthesis as the basis of synergism of methotrexate and 6-mercaptopurine in human malignant lymphoblasts of different lineages. *Biochem Pharmacol* 37:2321-2327.

32. Beckers, A., Organe, S., Timmermans, L., Vanderhoydonc, F., Deboel, L., Derua, R., Waelkens, E., Brusselmans, K., Verhoeven, G., and Swinnen, J.V. 2006. Methotrexate enhances the antianabolic and antiproliferative effects of 5-aminoimidazole-4-carboxamide riboside. *Mol Cancer Ther* 5:2211-2217.

33. Kaminskas, E., and Nussey, A.C. 1978. Effects of methotrexate and of environmental factors on glycolysis and metabolic energy state in cultured Ehrlich ascites carcinoma cells. *Cancer Res* 38:2989-2996.

34. Oakhill, J.S., Steel, R., Chen, Z.P., Scott, J.W., Ling, N., Tam, S., and Kemp, B.E. 2011. AMPK is a direct adenylate charge-regulated protein kinase. *Science* 332:1433-1435.

35. Davies, S.P., Helps, N.R., Cohen, P.T., and Hardie, D.G. 1995. 5'-AMP inhibits dephosphorylation, as well as promoting phosphorylation, of the AMP-activated protein kinase. Studies using bacterially expressed human protein phosphatase-2C alpha and native bovine protein phosphatase-2AC. *FEBS Lett* 377:421-425.

36. Mahlapuu, M., Johansson, C., Lindgren, K., Hjalm, G., Barnes, B.R., Krook, A., Zierath, J.R., Andersson, L., and Marklund, S. 2004. Expression profiling of the gamma-subunit isoforms of AMP-activated protein kinase suggests a major role for gamma3 in white skeletal muscle. *Am J Physiol Endocrinol Metab* 286:E194-200.

37. Scott, J.W., van Denderen, B.J., Jorgensen, S.B., Honeyman, J.E., Steinberg, G.R., Oakhill, J.S., Iseli, T.J., Koay, A., Gooley, P.R., Stapleton, D., et al. 2008. Thienopyridone drugs are selective activators of AMP-activated protein kinase beta1-containing complexes. *Chem Biol* 15:1220-1230.

38. Wojtaszewski, J.F., Birk, J.B., Frosig, C., Holten, M., Pilegaard, H., and Dela, F. 2005. 5'AMP activated protein kinase expression in human skeletal muscle: effects of strength training and type 2 diabetes. *J Physiol* 564:563-573.

39. Cuthbertson, D.J., Babraj, J.A., Mustard, K.J., Towler, M.C., Green, K.A., Wackerhage, H., Leese, G.P., Baar, K., Thomason-Hughes, M., Sutherland, C., et al.

2007. 5-aminoimidazole-4-carboxamide 1-beta-D-ribofuranoside acutely stimulates skeletal muscle 2-deoxyglucose uptake in healthy men. *Diabetes* 56:2078-2084.

40. Cheung, P.C., Salt, I.P., Davies, S.P., Hardie, D.G., and Carling, D. 2000. Characterization of AMP-activated protein kinase gamma-subunit isoforms and their role in AMP binding. *Biochem J* 346 Pt 3:659-669.

41. Birk, J.B., and Wojtaszewski, J.F. 2006. Predominant alpha2/beta2/gamma3 AMPK activation during exercise in human skeletal muscle. *J Physiol* 577:1021-1032.

42. Garcia-Roves, P.M., Osler, M.E., Holmstrom, M.H., and Zierath, J.R. 2008. Gain-of-function R225Q mutation in AMP-activated protein kinase gamma3 subunit increases mitochondrial biogenesis in glycolytic skeletal muscle. *J Biol Chem* 283:35724-35734.

43. Wang, Y.C., and Chiang, E.P. 2012. Low-dose methotrexate inhibits methionine S-adenosyltransferase in vitro and in vivo. *Mol Med* 18:423-432.

44. Martinez-Chantar, M.L., Vazquez-Chantada, M., Garnacho, M., Latasa, M.U., Varela-Rey, M., Dotor, J., Santamaria, M., Martinez-Cruz, L.A., Parada, L.A., Lu, S.C., et al. 2006. S-adenosylmethionine regulates cytoplasmic HuR via AMP-activated kinase. *Gastroenterology* 131:223-232.

45. Hornik, P., Vyskocilova, P., Friedecky, D., and Adam, T. 2006. Diagnosing AICA-ribosiduria by capillary electrophoresis. *J Chromatogr B Analyt Technol Biomed Life Sci* 843:15-19.

46. Holmes, B.F., Kurth-Kraczek, E.J., and Winder, W.W. 1999. Chronic activation of 5'-AMP-activated protein kinase increases GLUT-4, hexokinase, and glycogen in muscle. *J Appl Physiol* 87:1990-1995.

47. Sugita, T., Aya, H., Ueno, M., Ishizuka, T., and Kawashima, K. 1997. Characterization of molecularly cloned human 5-aminoimidazole-4-carboxamide ribonucleotide transformylase. *J Biochem* 122:309-313.

48. Chan, E.S., Montesinos, M.C., Fernandez, P., Desai, A., Delano, D.L., Yee, H., Reiss, A.B., Pillinger, M.H., Chen, J.F., Schwarzschild, M.A., et al. 2006. Adenosine A(2A) receptors play a role in the pathogenesis of hepatic cirrhosis. *Br J Pharmacol* 148:1144-1155.

49. Worm, J., Kirkin, A.F., Dzhandzhugazyan, K.N., and Guldberg, P. 2001. Methylation-dependent silencing of the reduced folate carrier gene in inherently methotrexate-resistant human breast cancer cells. *J Biol Chem* 276:39990-40000.

FIGURE LEGENDS

Figure 1. MTX promotes AMPK activation in cultured myotubes. (A, B) Phosphorylation of AMPK (at Thr^{172}) and its target (C, D) ACC (at Ser^{79}) were determined in L6 myotubes and in primary human myotubes (HSMC) upon exposure to 5 μM MTX and/or 0.2 mM or 2 mM AICAR (5 hr). Myotubes were preincubated with 5 μM MTX or vehicle for 16 hr prior to the experiment. Results are means ± SEM (n=6). #P<0.05 vs. Basal, *P<0.05 vs. AICAR (0.2 mM).

Figure 2. MTX promotes metabolic effects in skeletal muscle via AMPK activation. (A) Palmitate oxidation (n=7-8, except Basal and MTX, where n=15) and (B) glucose uptake (n=24) in L6 myotubes upon exposure to 5 μM MTX and/or 0.2 mM or 2 mM AICAR (5 hr). L6 myotubes were preincubated with 5 μM MTX or vehicle for 16 hr prior to the palmitate oxidation or glucose uptake assay. (C) Glucose uptake in isolated EDL (black bars) and soleus (white bars) muscle after exposure to 10 μM MTX, 120 nM insulin and/or 2 mM AICAR (n=6-8). EDL and soleus muscle were preincubated with 10 μM MTX or vehicle for 2 hr prior to the glucose uptake assay. Results are means ± SEM. #P<0.05 vs. Basal, *P<0.05 vs. AICAR (0.2 mM) or as indicated.

Figure 3. MTX promotes AMPK activation through indirect mechanisms. (A) ZMP content and (B) the ADP:ATP ratio in L6 myotubes exposed to 5 μM MTX and/or 0.2 mM AICAR (5 hr). L6 myotubes were preincubated with 5 μM MTX or vehicle for 16 hr prior to the experiment. Results are means ± SEM (n=3-5). (C) ZMP content and (D) the ADP:ATP ratio in WT cells exposed to 3 μM MTX and/or different concentrations of AICAR. Means ± SD (n=2). Activity of AMPK in (E) WT cells and (F) RG cells exposed to 3 μM MTX and/or different concentrations of AICAR (1 hr). WT and RG cells were preincubated with 3 μM MTX (black circles) or vehicle (white circles) for 16 hr prior to the AMPK activity assay. Results are means ± SEM (n=2-4). AMPK activity is expressed as percentage of the activity in controls without added treatments. Results are means ± SEM (n=11-12). *P<0.05 vs. without MTX or as indicated.

Figure 4. MTX is not a direct AMPK activator. (A) Activity of purified rat liver AMPK was measured following incubation with increasing concentrations of MTX in the absence (white bars) or presence (black bars) of 200 μM AMP. (B) Activity of purified rat liver AMPK before (white bars)

and after 10-minute incubation with PP2C (black bars) in the presence or absence of MTX (1-30 μM) or 200 μM AMP. AMPK activities are expressed as percentages of activity in the controls without added treatments. Results are means ± SD (n=2).

Figure 5. MTX is dependent on AMPK to promote lipid oxidation in isolated skeletal muscle. (A, B) Phosphorylation of AMPK and (C, D) its target ACC and (E, F) palmitate oxidation were measured in wild-type (black bars) or AMPK-$\gamma3^{-/-}$ (white bars) EDL and soleus muscle after exposure to 10 μM MTX and/or 0.2 mM AICAR (2 hr). EDL and soleus muscle were preincubated with 10 μM MTX or vehicle for 2 hr prior to the experiment. Results are means ± SEM (n=12). **P*<0.05 vs. AICAR

Figure 6. Suppression of ATIC promotes AMPK activation and increases lipid oxidation in L6 myotubes by a direct mechanism. (A) ATIC expression was determined by immunoblot in L6 myotubes, differentiated primary human skeletal muscle cells (HSMC), HEK-293 cells and in murine EDL and soleus muscle. (B) ATIC protein expression in L6 myotubes after transfection with scrambled siRNA (Scr) or siRNA against ATIC (siATIC). (C) ZMP content, (D) the ADP:ATP ratio, (E) AMPK phosphorylation, (F) ACC phosphorylation and (G) palmitate oxidation measured in control or ATIC-depleted L6 myotubes upon exposure to 0.2 mM AICAR (5 hr). Results for nucleotide measurements are means for Basal (n=2) and means ± SEM (n=4) for AICAR. For all others results are means ± SEM (n=8). #P<0.05 vs. Basal (Scr), *P<0.05 vs. AICAR (Scr). (H-J) ATIC-depleted or control L6 myotubes were preincubated with 5 μM MTX for 16 hr. (H) AMPK phosphorylation, (I) ACC phosphorylation and (J) palmitate oxidation were determined upon exposure to 0.2 mM AICAR (5 hr). Results are means ± SEM (n=6). **P*<0.05 vs. MTX (Scr).

Figure 7. MTX promotes AMPK activation in skeletal muscle through different mechanisms. Clearance of AICAR through the *de novo* purine synthesis pathway limits effectiveness of AICAR as an AMPK activator in skeletal muscle. Co-therapy with AICAR and MTX may overcome these limitations by reducing the threshold for AMPK activation in skeletal muscle. Underlying mechanisms include diminished ZMP clearance and energy deprivation. However, other ATIC-independent mechanisms are likely involved. AICA: 5-aminoimidazole-4-carboxamide, GART: glycinamide

ribonucleotide transformylase, IMP: inosine monophosphate, PRPP: 5-phosphoribosyl-1-pyrophosphate.

Table 1 ***Effect of MTX on ZMP content and adenylate energy charge in AICAR-treated murine skeletal muscle.***

Skeletal muscle	Treatment	ZMP:ATP	Adenylate energy charge
EDL	**AICAR**	0.041 ± 0.002	0.93 ± 0.005
	MTX + AICAR	0.039 ± 0.002	0.92 ± 0.01
Soleus	**AICAR**	0.12 ± 0.013	0.80 ± 0.04
	MTX + AICAR	0.12 ± 0.016	0.80 ± 0.05

ZMP content, expressed as the ZMP:ATP ratio, and adenylate energy charge, calculated as ([ATP] + 0.5[ADP]) / ([ATP] + [ADP] + [AMP]), were determined in wild-type EDL and soleus muscle after exposure to 0.2 mM AICAR and 10 μM MTX (2 hr). EDL and soleus muscle were preincubated with 10 μM MTX or vehicle for 2 hr prior to the experiment. ZMP was below detection limit under basal conditions (data not shown). Results are means ± SEM (n=3-4).

Figure 1

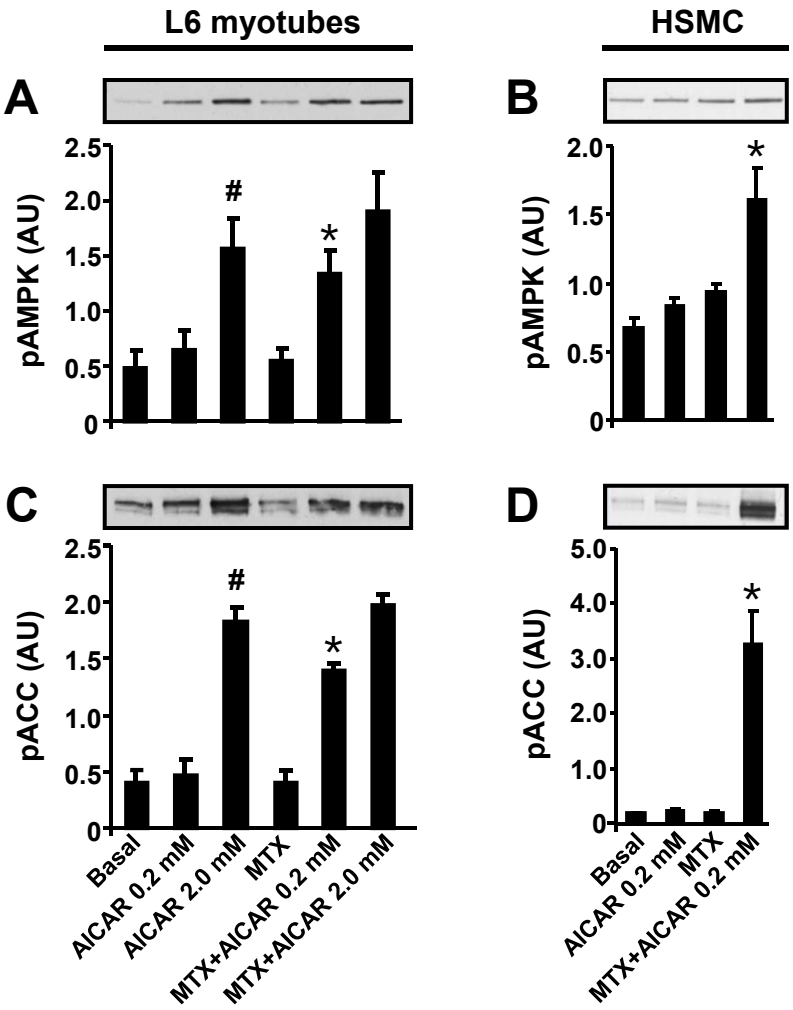
L6 myotubes
HSMC
A
B
C
D
pAMPK (AU)
pACC (AU)
#
*
Basal
AICAR 0.2 mM
AICAR 2.0 mM
MTX
MTX+AICAR 0.2 mM
MTX+AICAR 2.0 mM

Figure 2

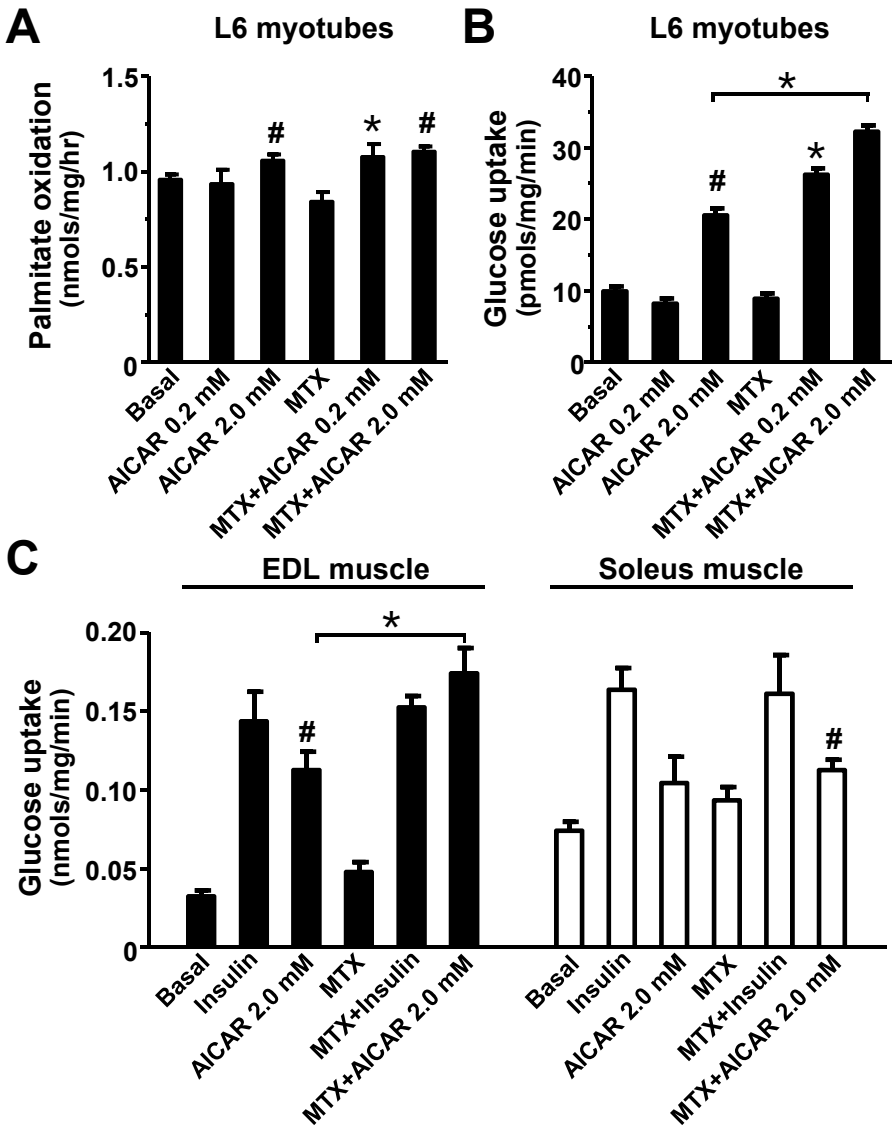
A
L6 myotubes
Palmitate oxidation (nmols/mg/hr)
1.5
1.0
0.5
0
#
*
#
Basal
AICAR 0.2 mM
AICAR 2.0 mM
MTX
MTX+AICAR 0.2 mM
MTX+AICAR 2.0 mM
B
L6 myotubes
Glucose uptake (pmols/mg/min)
40
30
20
10
0
*
#
*
Basal
AICAR 0.2 mM
AICAR 2.0 mM
MTX
MTX+AICAR 0.2 mM
MTX+AICAR 2.0 mM
C
EDL muscle
Soleus muscle
Glucose uptake (nmols/mg/min)
0.20
0.15
0.10
0.05
0
*
#
#
Basal
Insulin
AICAR 2.0 mM
MTX
MTX+Insulin
MTX+AICAR 2.0 mM
Basal
Insulin
AICAR 2.0 mM
MTX
MTX+Insulin
MTX+AICAR 2.0 mM

Figure 3

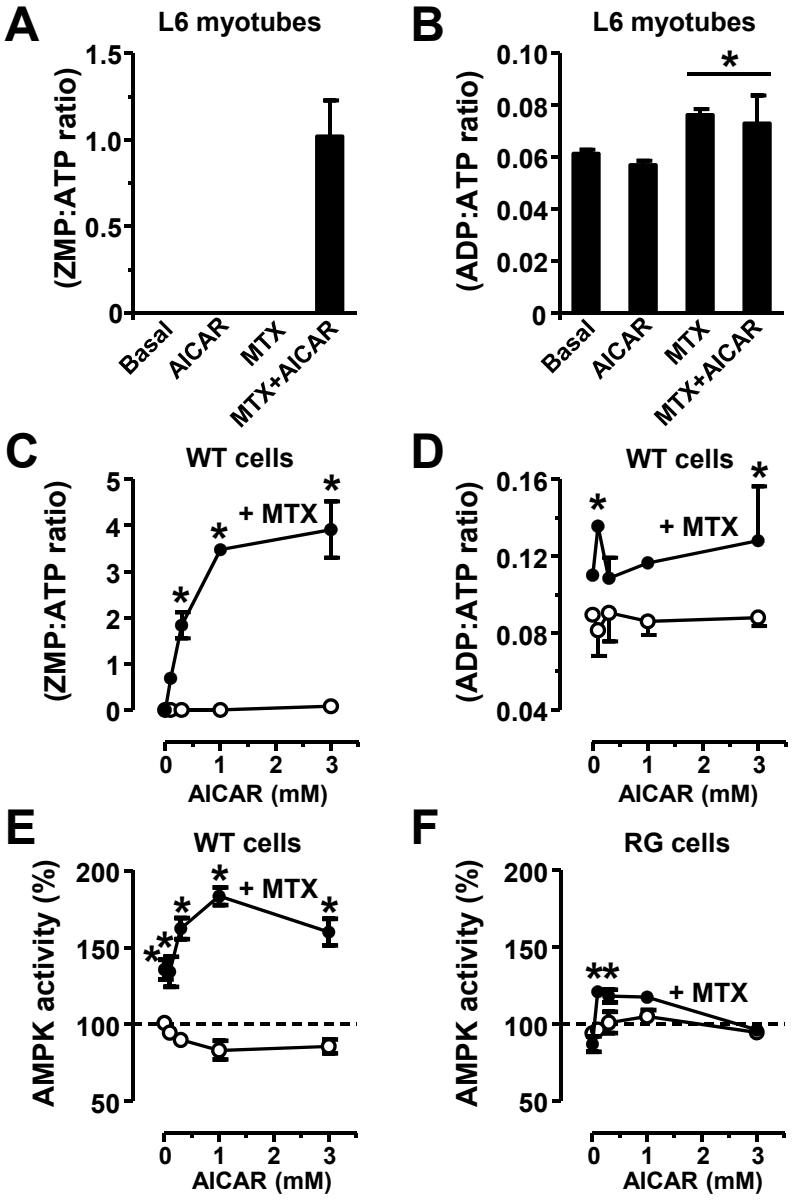
A
L6 myotubes
(ZMP:ATP ratio)
1.5
1.0
0.5
0
Basal
AICAR
MTX
MTX+AICAR
B
L6 myotubes
(ADP:ATP ratio)
0.10
0.08
0.06
0.04
0.02
0
*
Basal
AICAR
MTX
MTX+AICAR
C
WT cells
(ZMP:ATP ratio)
+ MTX
AICAR (mM)
D
WT cells
(ADP:ATP ratio)
+ MTX
AICAR (mM)
E
WT cells
AMPK activity (%)
+ MTX
AICAR (mM)
F
RG cells
AMPK activity (%)
+ MTX
AICAR (mM)

Figure 4

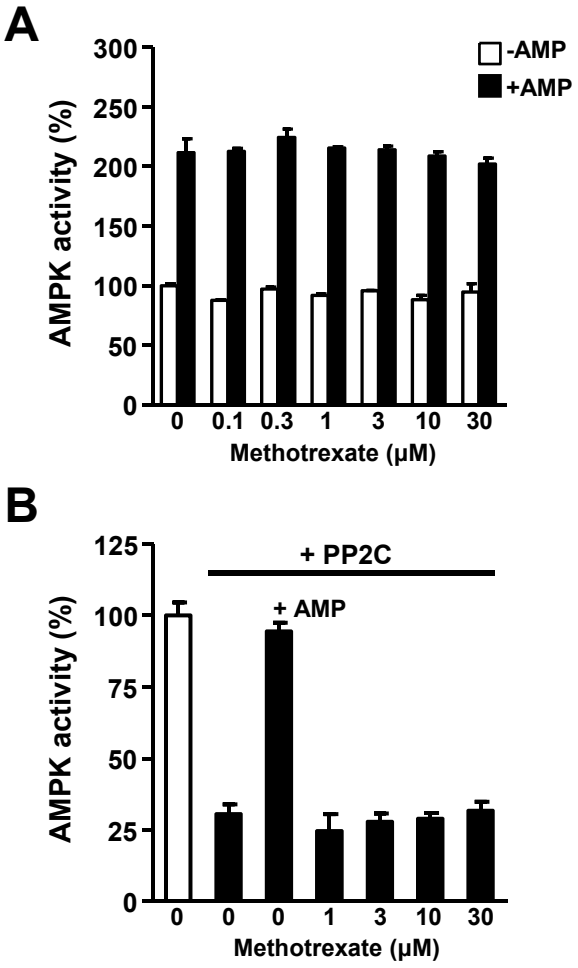
A
-AMP
+AMP
AMPK activity (%)
300
250
200
150
100
50
0
0 0.1 0.3 1 3 10 30
Methotrexate (μM)
B
+ PP2C
+ AMP
AMPK activity (%)
125
100
75
50
25
0
0 0 0 1 3 10 30
Methotrexate (μM)

Figure 5

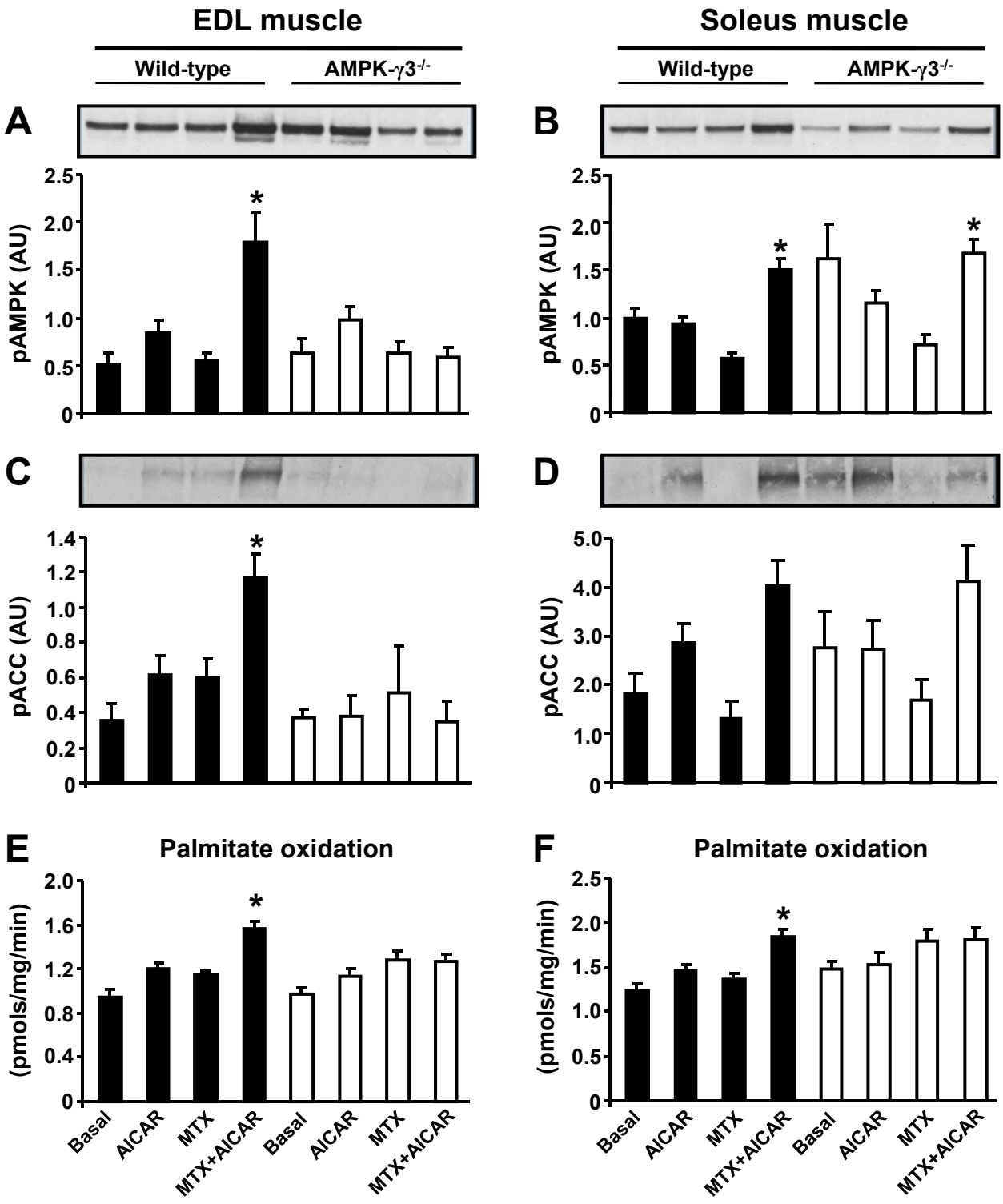
EDL muscle
Soleus muscle
Wild-type
AMPK-γ3-/-
A
B
C
D
E
F
pAMPK (AU)
pACC (AU)
Palmitate oxidation
(pmols/mg/min)
Basal
AICAR
MTX
MTX+AICAR

Figure 6

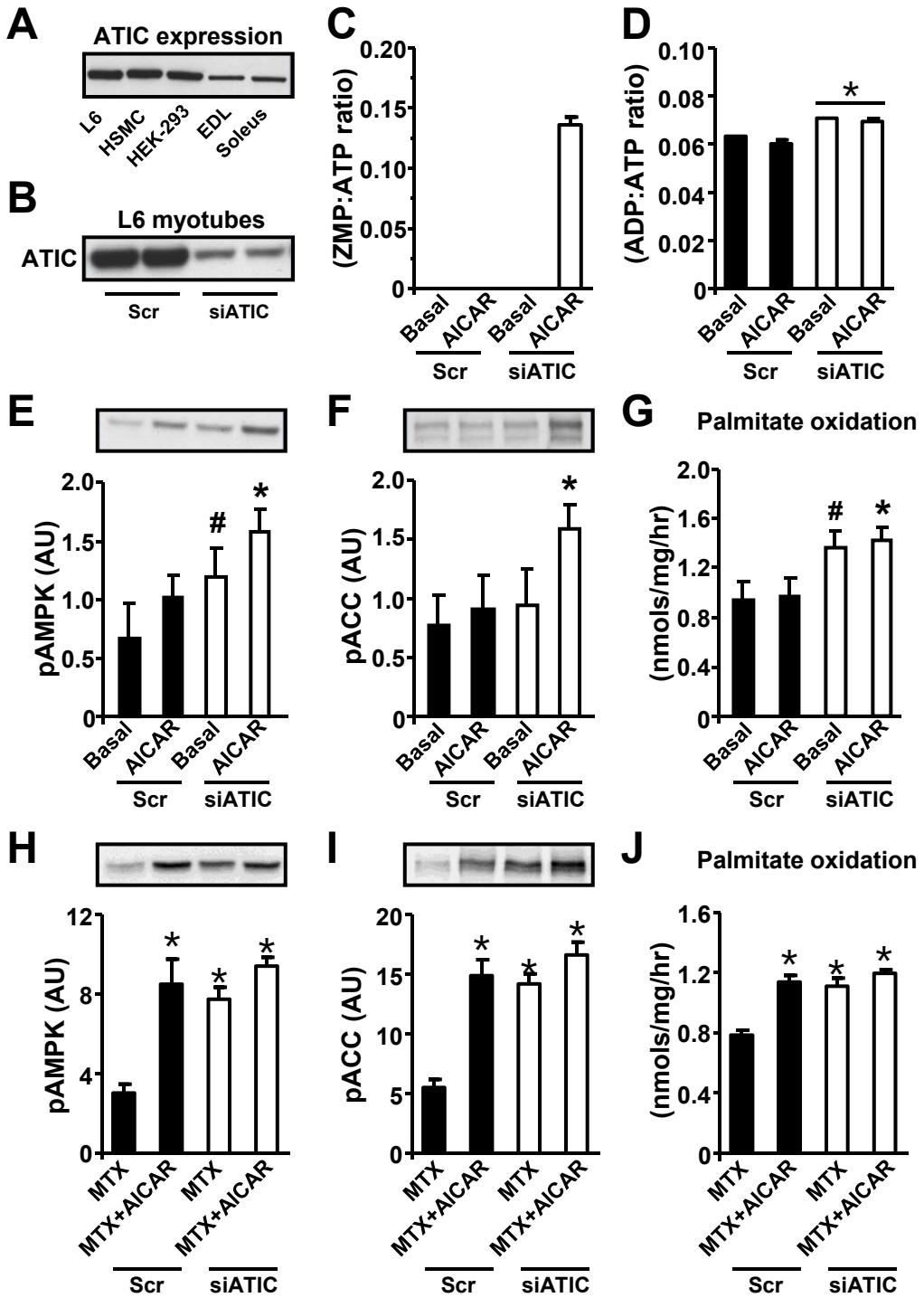
A
ATIC expression
L6
HSMC
HEK-293
EDL
Soleus
B
L6 myotubes
ATIC
Scr
siATIC
C
(ZMP:ATP ratio)
0.20
0.15
0.10
0.05
0
Basal
AICAR
Basal
AICAR
Scr
siATIC
D
(ADP:ATP ratio)
0.10
0.08
0.06
0.04
0.02
0
*
Basal
AICAR
Basal
AICAR
Scr
siATIC
E
pAMPK (AU)
2.0
1.5
1.0
0.5
0
#
*
Basal
AICAR
Basal
AICAR
Scr
siATIC
F
pACC (AU)
2.0
1.5
1.0
0.5
0
*
Basal
AICAR
Basal
AICAR
Scr
siATIC
G
Palmitate oxidation
(nmols/mg/hr)
2.0
1.6
1.2
0.8
0.4
0
#
*
Basal
AICAR
Basal
AICAR
Scr
siATIC
H
pAMPK (AU)
12
8
4
0
*
*
*
MTX
MTX+AICAR
MTX
MTX+AICAR
Scr
siATIC
I
pACC (AU)
20
15
10
5
0
*
*
*
MTX
MTX+AICAR
MTX
MTX+AICAR
Scr
siATIC
J
Palmitate oxidation
(nmols/mg/hr)
1.6
1.2
0.8
0.4
0
*
*
*
MTX
MTX+AICAR
MTX
MTX+AICAR
Scr
siATIC

Figure 7

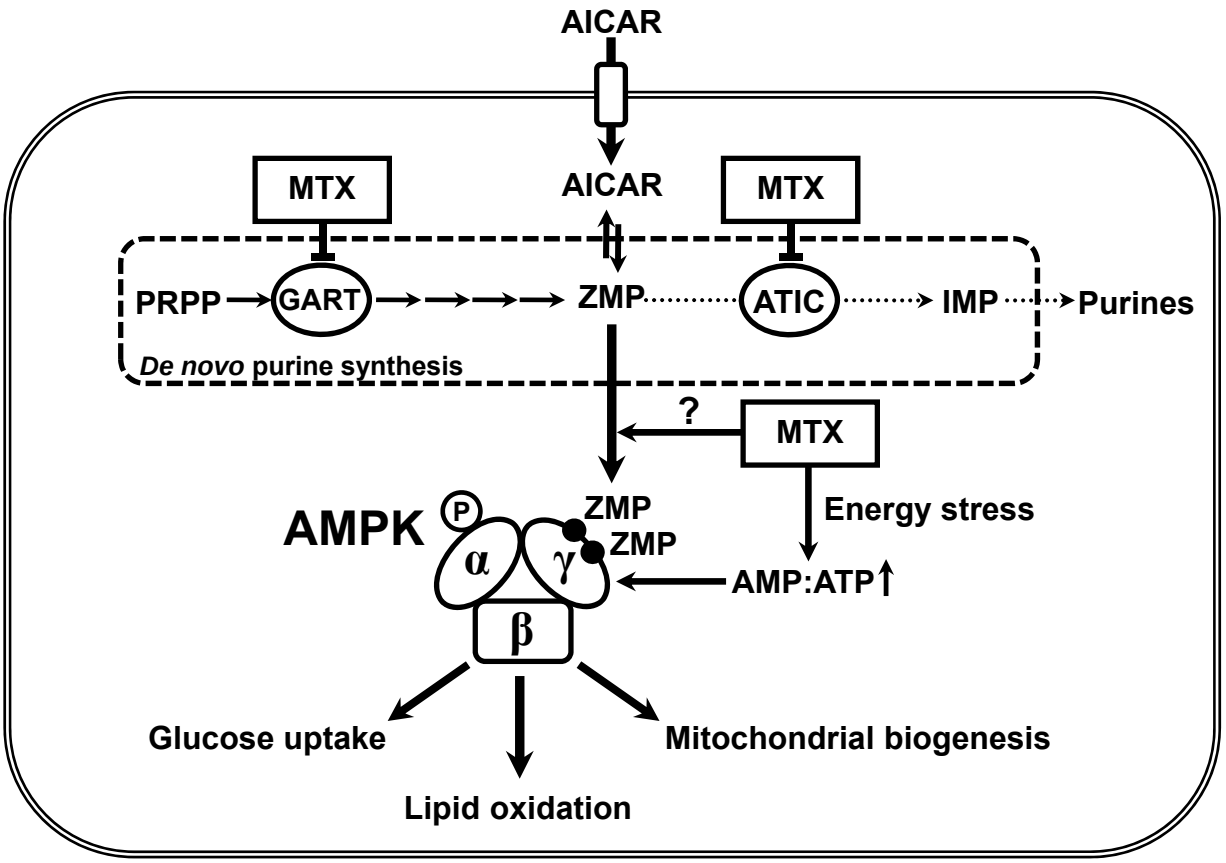
AICAR
AICAR
MTX
MTX
PRPP
GART
ZMP
ATIC
IMP
Purines
De novo purine synthesis
?
MTX
AMPK
P
α
γ
β
ZMP
ZMP
Energy stress
AMP:ATP
Glucose uptake
Mitochondrial biogenesis
Lipid oxidation